Dalton Transactions

Inducing selectivity and chirality in group IV metal coordination with high-denticity hydroxypyridinones

Journal:	*Dalton Transactions*
Manuscript ID	DT-ART-03-2019-001031.R1
Article Type:	Paper
Date Submitted by the Author:	20-Apr-2019
Complete List of Authors:	Deblonde, Gauthier; Lawrence Berkeley National Laboratory Lohrey, Trevor; University of California Berkeley Abergel, Rebecca; University of California Berkeley; Lawrence Berkeley National Laboratory

Journal Name

ARTICLE

Inducing selectivity and chirality in group IV metal coordination with high-denticity hydroxypyridinones

Received 00th January 20xx,
Accepted 00th January 20xx

DOI: 10.1039/x0xx00000x

www.rsc.org/

Gauthier J.-P. Deblonde,[a] Trevor D. Lohrey[a,b] and Rebecca J. Abergel*[a,c]

The solution- and solid-state interactions between the octadentate siderophore mimic 3,4,3-LI(1,2-HOPO) (343HOPO) and group IV metal ions were investigated using high-resolution mass spectrometry, liquid chromatography, UV-visible spectrophotometry, metal-competition batch titrations, and single crystal X-ray diffraction. 343HOPO forms a neutral 1:1 complex, [Hf^{IV}343HOPO], that exhibits extreme stability in aqueous solution, with a log β_{110} value reaching 42.3. These results affirm the remarkable charge-based selectivity of 343HOPO for octacoordinated tetravalent cations with a Hf(IV) complex 10^{21} more stable than its Lu(III) analogue. Moreover, [Hf^{IV}343HOPO] and its Zr(IV) counterpart show exceptional robustness, with the ligand remaining bound to the cation over a very broad pH range: from pH ~11 to acidic conditions as strong as 10 M HCl. In stark contrast, Ti(IV)-343HOPO species are far less stable and undergo hydrolysis at pH as low as ~6, likely due to the mismatch between the preferred hexacoordinated Ti(IV) ion and octadentate 343HOPO ligand. The extreme charge-based and denticity-driven selectivity of 343HOPO, now observed accros the periodic table, paves the way for new selective sequestration systems for radionuclides including medical ^{44}Ti, ^{89}Zr or ^{177}Lu/Hf isotopes, toxic polonium (Po) contaminants, as well as rutherfordium (Rf) research isotopes. Furthermore, despite the lack of a chiral center in 343HOPO, its complexes with metal ions are chiral and appear to form a single set of enantiomers.

Introduction

Octadentate siderophore derivative 3,4,3-LI(1,2-HOPO) (hereafter "343HOPO") was first synthesized in the late 1980's and was originally designed for the sequestration of Pu in the context of decontamination treatments following internal contamination with radionuclides.[1,2] Since then, this negatively charged ligand has been studied for its sensitization and/or chelation properties with various cations such as divalent uranyl, Cd, and Pb ions[3,4], trivalent lanthanide fission products and trivalent actinides[5–7], as well as tetravalent Zr, Sn, Ce, Th, and Bk[4,8–11].

The solution chemistry of Hf is often considered similar to that of Zr and can, sometimes, be overlooked. 343HOPO has recently shown promises for use as Zr(IV) chelator for Zr-89 positron emission tomography (PET) imaging.[11,12] The interactions between Hf(IV) and 343HOPO (that bears up to four negative charges when deprotonated - Fig. 1) had never been probed despite some overlap between the clinical use Hf and the biomedical development of this ligand. Hf-based pharmaceuticals are instrumental to the medical community and there is great need for water-soluble, strong and robust chelators that bind Hf(IV) *in vitro* and *in vivo*. For example, a new class of Hf(IV)-azainositol complexes has recently been developed for X-Ray computed tomography (CT) imaging.[13,14] Hf is also important to the development of anti-cancer treatments such as targeted radioimmunotherapies involving the radionuclide Lu-177 (Half-life of 6.6 days, β^-, $E_{\beta max}$ = 497 keV, 384 keV, and 176 keV)[15]. In fact, during target irradiation, Lu atoms absorb neutrons, which leads to formation of the stable isotopes Hf-177 and Hf-178 as by-products. Accumulation of Hf isotopes in the Lu target therefore decreases the specific activity of the material. Furthermore, radioactive Lu-177 quickly decays to stable Hf-177 so that the production of Lu-177 sources with a high specific activity (*i.e.* career-free Lu-177) necessitates the separation of Lu(III) and Hf(IV) ions.

Likewise, some Ti isotopes are also indirectly or directly useful to the medical world. For example, Ti-44 (Half-life of 60.2 years, ε) is used in one of the two main routes of production of Sc-44 (Half-life of 3.97 hours, β^+) for PET imaging, via Ti-44/Sc-44 generators.[16,17] Ti-45 (Half-life of 3.1 hours, β^+) is also used for PET imaging[18] and, similar to Lu/Hf systems, Ti isotope production necessitates the separation of Sc(III) and Ti(IV) ions. Building upon previous studies on metal-ligand complexes formed with 343HOPO, this work probes interactions, both in the solid- and solution-state, between 343HOPO and the group IV metal ions as well as other relevant cations. These systems demonstrate 343HOPO's unmatched charge-based selectivity and denticity-driven chelation and also reveal the previously undiscussed chiral features of the 343HOPO-metal complexes.

a. *Chemical Sciences Division, Lawrence Berkeley National Laboratory, Berkeley, CA 94720, USA.*
b. *Department of Chemistry, University of California, Berkeley, CA 94720, USA.*
c. *Department of Nuclear Engineering, University of California, Berkeley, CA 94720, USA. Email: abergel@berkeley.edu*

Electronic Supplementary Information (ESI) available: [details of any supplementary information available should be included here]. See DOI: 10.1039/x0xx00000x

Experimental

Chemicals. The ligand 3,4,3-LI(1,2-HOPO) was synthesized and characterized as previously described.[19] N-Cyclohexyl-2-aminoethanesulfonic acid ("CHES", >99%, Sigma-Aldrich), 4-(2-hydroxyethyl)-1-piperazineethanesulfonic acid ("HEPES", 99%, Sigma-Aldrich), KCl (> 99.9995%, Sigma-Aldrich), potassium hydrogen phthalate (99.95%, Sigma-Aldrich), $ZrCl_4$ (99.99%, Sigma-Aldrich), $HfCl_4$ (99.5%, VWR) were used as received. Metal stock solutions were prepared by direct dissolution of the high purity salts in standard 2 M HCl solutions. Zr and Hf salts were weighted under argon atmosphere. $TiCl_4$ standard solutions were purchased from Fluka Analytical. Carbonate-free 0.1 M KOH was prepared from Baker *Dilut-It* concentrate and was standardized by titrating against 0.1 M potassium hydrogen phthalate. Standard solutions of HCl were purchased from VWR. All solutions were prepared using deionized water purified by a Millipore Milli-Q reverse osmosis cartridge system. Stocks were stored at 2-8°C in the dark between experiments.

Instrumentation. The glass electrode (Metrohm - *Micro Combi* - response to $[H^+]$) used for the pH measurements was calibrated at 25.0°C and at an ionic strength of 0.1M (KCl) before each titration. The calibration data were analyzed using the program GLEE to refine for the slope and E^0.[20] The automated titration system was controlled by an 867 pH Module (Metrohm). Two-milliliter Dosino 800 burets (Metrohm) dosed the titrant (standard 0.1 M KOH or 0.1 M HCl) into the thermostated titration vessel (5–90 mL). UV–visible spectra were acquired with an Ocean Optics USB4000-UV–vis spectrophotometer equipped with a TP-300 dip probe (Ocean Optics, 10 mm path length), fiber optics and a DH-2000 light source (deuterium and halogen lamps). The automated titration system and the UV-vis spectrophotometer were coordinated by the LBNL titration system program, developed in-house. Static UV–visible spectra were measured using a Cary 5G spectrophotometer.

Liquid chromatography. Retention times of the 343HOPO complexes with Sn(IV), Zr(IV), and Hf(IV) were measured with a C18 column (Agilent Technologies, Zorbax Eclipse column XDB-C18, 5 µm, 4.6 × 150 mm) on an Ultra Performance Liquid Chromatography (UPLC) Waters Xevo system (Waters Corporation, Milford, MA, USA). LC traces are provided in Figure S1. The free ligand 343HOPO was used as a reference. The instrument and elution conditions were the same as those previously optimized by Sturzbecher-Hoehne et al.[8] The new results for Zr(IV) and the free ligand are in perfect agreement with results reported by Sturzbecher-Hoehne et al.

High resolution mass spectrometry. High resolution mass spectra (HRMS) were acquired on a UPLC Waters Xevo system interfaced with a QTOF mass spectrometer (Waters Corporation, Milford, MA, USA) in Micromass Z-spray geometry (Figure S1). The mass spectrometer was equipped with an ESI source. Data acquisition and instrument control were accomplished using MassLynx software, version 4.1. Aqueous solutions containing 25 µM of the ligand and the metal of interest (metal/ligand = 1 mol/mol) were directly injected at a flow of 20 $\mu L.min^{-1}$ using a syringe pump (KD Scientific, Holliston, MA, USA). The voltage applied to the capillary was 3.00 and 2.50 kV in the positive and negative detection modes, respectively. A nitrogen gas flow rate of 30 L/h was used for the cone and 600 L/h for desolvation. The cone voltage was set to 20 V in positive mode and 40 V in negative mode. The temperature was 80°C for the ion source and 375°C for desolvation. Mass spectra were recorded over a 200−1400 m/z range over collection times of 1 min.

Incremental spectrophotometric titrations. Typically, a solution (9 mL) containing ligand (40 µM), metal of interest (40 µM), and supporting electrolyte, was incrementally perturbed by addition of 0.010 mL of 0.1 M KOH followed by a time delay of 60 s. The measurements were done once a stable pH value was reached. Buffering of the solution was assured by the addition of HEPES, CHES and acetic acid (≤ 3 mM). Between 110 and 190 data points were collected per titration, each data point consisting of a volume increment (0.010 mL), an electrode potential measurement, and an absorbance spectrum (260-750 nm, at intervals of approximately 0.2 nm). Titrations were performed from pH ~2 to ~12 and at an ionic strength of 0.1 M.

Metal competition batch titrations. Series of samples containing typically 20-50 µM of 343HOPO, 1.00 equivalent of $HfCl_4$ and from 0 to 2.00 equivalent of $ZrCl_4$ were prepared in 0.4 M HCl. Each series contained at least 10 samples that were equilibrated for 48 hours at 20°C in a thermostated bath. UV-visible spectra were recorded at equilibrium. At least three independent titrations were performed. The reported uncertainty corresponds to the standard deviation observed over three independent procedures; each procedure consisting of sample preparation, measurements, and data treatment.

Titration data treatment. Spectrophotometric titration data sets were imported into the refinement program HypSpec[21] and analyzed by nonlinear least-squares refinement. All equilibrium constants were defined as cumulative formation constants, β_{mlh} according to Eq. 1 and Eq. 2, where the metal and ligand are designated as M and L, respectively.

$$m\mathrm{M} + h\mathrm{H} + l\mathrm{L} \rightleftharpoons [\mathrm{M}_m\mathrm{H}_h\mathrm{L}_l] \qquad \text{Eq. 1}$$

$$\beta_{mlh} = \frac{[\mathrm{M}_m\mathrm{H}_h\mathrm{L}_l]}{[\mathrm{M}]^m[\mathrm{H}]^h[\mathrm{L}]^l} \qquad \text{Eq. 2}$$

For species containing hydroxides, the h value is negative. All metal and ligand total concentrations were held at estimated values determined from the volume of standardized stock solutions. All species formed with 343HOPO were considered to have absorbance significant enough to be observed in the UV-vis spectra and were therefore included in the refinement process. The chemical equilibria taken into account were as follows: autoprotolysis of water, ligand protonation, ligand-metal complexation, metal hydroxide formation, and metal chloride complexes formation (due to the presence of chloride in the background electrolyte). The hydroxide and chloride complex formation constants were taken from the NIST[22] or OECD[23,24] databases. The list of the stability constants fixed during the refinement processes is given in Table S1.

Crystallography. Single crystals, suitable for X-ray diffraction, of the Hf(IV) complex were obtained by slow evaporation of samples initially containing 6 mM of $HfCl_4$ and 6 mM of

343HOPO in ethanol:water (85:15). Samples were incubated at 55°C for 60 min before filtration and slow evaporation. Crystals formed over at least 3 weeks at room temperature. Several of these crystals were transferred from their mother liquor, suspended in Paratone® oil, and inspected under a microscope equipped with a polarizing filter. The crystals were cut into pieces of appropriate size, and a colorless shard of dimensions 0.10 x 0.08 x 0.06 mm^3 was selected and mounted onto a 10-micron MiTiGen dual thickness MicroMount™. The mounted crystal was then immediately placed on the goniometer head of the diffractometer and cooled in a 100-K stream of dry N_2.

Table 1 Crystallographic data and structure refinement for the Hf(IV) complex of 343HOPO.

	$[Hf^{IV}343HOPO]\cdot 3H_2O$
Chemical formula	$C_{34}H_{40}N_8O_{15}Hf$
Formula weight	979.23
Color, habit	Colorless, shard
Temperature (K)	100(2)
Crystal system	Orthorhombic
Space group	$C222_1$
a (Å)	16.0989(7)
b (Å)	16.9738(7)
c (Å)	13.3829(6)
α (°)	90
β (°)	90
γ (°)	90
V ($Å^3$)	3657.0(3)
Z	4
Density (Mg m^{-3})	1.779
F(000)	1968
Radiation Type	Synchrotron
μ (mm^{-1})	3.582
Crystal size (mm^3)	0.100 x 0.080 x 0.060
Meas. Refl.	23773
Indep. Refl.	5551
R(int)	0.0229
Final R indices	R = 0.0211
[I > 2σ(I)]	R_w = 0.0558
Goodness-of-fit	1.047
Absolute structure parameter	0.027(3)
$\Delta\rho_{max}$, $\Delta\rho_{min}$ (e $Å^{-3}$)	3.052, -1.264

Data collection was conducted at the Advanced Light Source (ALS) station 11.3.1 at Lawrence Berkeley National Laboratory (LBNL), using a silicon-monochromated beam of 16 keV (λ = 0.7749 Å) synchrotron radiation. The Bruker APEX3 software package (including SAINT and SADABS) was used throughout data collection and reduction procedures.[25] The structure was determined and refined using SHELXT and SHELXL-2014 in the WinGX software package.[26,27] While the crystal analyzed and described in this work was largely single, several crystals of similar macroscopic properties were also analyzed and found to crystallize in the same space group, albeit with a much greater extent of inversion twinning.

Figures of the finalized structure were generated using Mercury.[28] CCDC 1891657 contains the supplementary crystallographic information for this paper. These data can be obtained free of charge from The Cambridge Crystallographic Data Centre. The crystallographic data and structure refinement of the Hf(IV) complex with 343HOPO are given in Table 1.

Results and discussion

Solution chemistry of group IV complexes with 343HOPO. The solution thermodynamics of the Hf(IV)-343HOPO and Ti(IV)-343HOPO systems had not yet been investigated. Previous reports[4,8–10] on 343HOPO complexes with tetravalent Sn, Ce, Th, Pu and Bk ions showed formation of 1:1 complexes. Herein, formation of neutral $[Hf^{IV}343HOPO]$ was confirmed by HRMS in positive mode (Figure S2). The mass spectrum of $[Hf^{IV}343HOPO]$ shows the expected isotopic pattern for a ^{nat}Hf compound and all the expected positive adducts for an aqueous complex, namely $[H\cdot Hf^{IV}343HOPO]^+$ (m/z = 927), $[Na\cdot Hf^{IV}343HOPO]^+$ (m/z = 949), and $[K\cdot Hf^{IV}343HOPO]^+$ (m/z = 955).

Based on the extremely high stability constant previously determined[8] for the corresponding Zr system (log β_{110} = 43.1 ±0.5), high stability was also expected for the Hf complex. The strong affinity of 343HOPO for tetravalent cations prevents determination of complex stability constants via classical techniques such as potentiometry, NMR, or calorimetry. Indirect methods must therefore be used like cyclic voltammetry (when the metal has another stable oxidation state), metal-exchange, or ligand-exchange using a competitor with established solution thermodynamics. Cyclic voltammetry is readily convenient for the determination of Ce(IV)/Ce(III) or Pu(IV)/Pu(III) complexes and this has been successfully applied to many chelators[9,29,30], including 343HOPO. The ligand exchange option has the advantage of preventing any metal hydrolysis issues, ubiquitous to very oxophilic cations such as Zr(IV) and Hf(IV), since the metal is always complexed by one of the two ligands engaged in the system. However, the ligand-exchange option necessitates a competing ligand whose affinity for the cation is in the same range (within a few orders of magnitude) as the studied ligand and its complex formation constants with the studied metal must also be known. The spectroscopic properties of the competing ligand must also be adequate to allow monitoring the reaction, which severely limits the ligand candidates. This option was only used[9] for colored $[Ce^{IV}343HOPO]$ species competing against transparent $[Ce(NTA)_2]^{2-}$ yielding results that were in good agreement with cyclic voltammetry. Unfortunately, the respective stability constants of the other potential $[M^{IV}(NTA)]_2]^{2-}$ (M = Ti, Zr, Hf, Sn ,Th, Pu, Bk) complexes are not known, so this method cannot currently be applied to other tetravalent complexes of 343HOPO. Consequently, metal exchange using $[Ce^{IV}343HOPO]$ as reference was used to determine the formation constants of the Zr, Th, and Pu complexes[8]. This inherently creates error propagation since the Ce(IV) complex is used as reference but it still is the only suitable method for determining the stability of preeminently stable 343HOPO complexes.

In order to directly compare the stability of $[Hf^{IV}343HOPO]$ with that of $[Zr^{IV}343HOPO]$, metal-exchange between Hf(IV) and Zr(IV) was employed (Fig. 1). Since Zr(IV) and Hf(IV) are prone to

hydrolysis, the metal exchange reaction was performed in acidic media (0.4 M HCl), as done previously for other hard Lewis acids[8,9]. Chloride complexation was therefore taken into account (Eq. 3), even if it has almost no effect on the 343HOPO complex formation constant value since chloride complexes of Zr(IV) and Hf(IV) have very similar stabilities[22] and are far less stable than 343HOPO species.

$$[Hf^{IV}343HOPO] + [Zr(Cl)_x]^{4-x} = [Zr^{IV}343HOPO] + [Hf(Cl)_y]^{4-y} + (x-y)\ Cl^- \quad \text{Eq. 3}$$

UV-vis spectra of pure [Hf^{IV}343HOPO] and [Zr^{IV}343HOPO] show slight yet significant differences so that the metal competition reaction can be followed by spectrophotometry (Figure S3). [Hf^{IV}343HOPO] exhibits the typical absorbance spectrum of aromatic 1,2-HOPO derivatives[9,31,32], with a π-π* transition centered at 300 nm. Interestingly, the wavelength of maximum absorbance, determined under identical conditions, seems correlated with the ionic radius of the metal center: 302 nm for Zr^{4+} (0.84 Å), 300 nm for Hf^{4+} (0.83 Å), and 299 nm for Sn^{4+} (0.81 Å). The extinction coefficient of [Hf^{IV}343HOPO] at 300 nm is 17,700 $M^{-1}.cm^{-1}$, which is almost identical to those of [Zr^{IV}343HOPO] (ε_{302} = 17,500 $M^{-1}.cm^{-1}$) and [Sn^{IV}343HOPO] (ε_{299} = 17,700 $M^{-1}.cm^{-1}$). Below 270 nm, the Hf complex extinction coefficient is also nearly identical to that of [Sn^{IV}343HOPO], whereas it is about 15 % lower than that of [Zr^{IV}343HOPO]. The absorption properties of [Sn^{IV}343HOPO] and [Hf^{IV}343HOPO] are very similar throughout the UV-vis domain and, for this particular reason, competition between the highly stable Sn(IV) complex (log β_{110} = 46.6 ±0.6)[4] and its Hf(IV) analogue cannot be used to reliably determine a formation constant.

Fig. 1 shows changes in UV-vis absorbance observed when Zr(IV) and Hf(IV) compete for octadentate 343HOPO. Upon increasing the ratio Zr/Hf from 0 to 2 equivalents, the π-π* band gradually shifts from 300 to 302 nm, two isosbestic points are observed at 277 and 301 nm, and the absorbance below 270 nm increases by about 15%. This is in line with spectra of the pure complexes and corresponds to a transmetallation from [Hf^{IV}343HOPO] to [Zr^{IV}343HOPO].

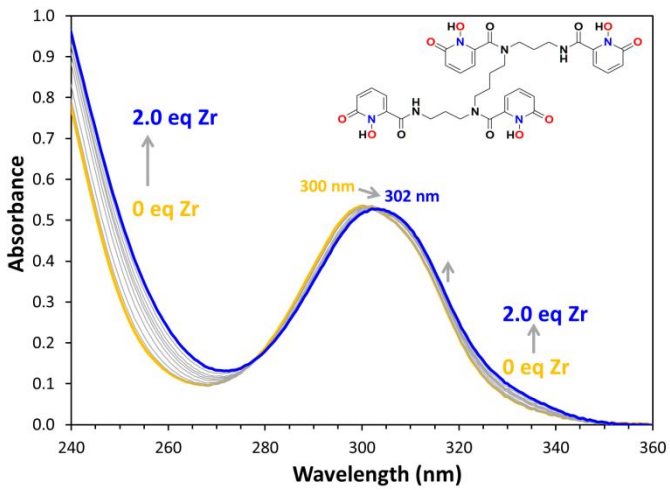

Fig. 1 Metal competition batch titration of [Hf^{IV}343HOPO)] against Zr(IV). [Hf] = [343HOPO] = 30 µM, $[Zr/Hf]_{total}$ = 0 to 2.0 mol/mol, I = 0.4 M (HCl), T = 20°C. Path length: 10 mm. Arrows highlight changes in absorbance due to metal exchange. The ligand formula is shown with its coordinating atoms highlighted in red.

This clearly indicates that Hf can be displaced by Zr and that 343HOPO has a higher affinity for the 4d cation than for the 5d metal ion. Refinement of the spectrophotometric titration data yielded a proton independent formation constant, log β_{110}, of 42.3 ±0.5 for [Hf^{IV}343HOPO]. This value is one order of magnitude lower than the previously reported value for the Zr complex (log β_{110}= 43.1 ±0.5). Given the high stability of the Hf complex and established robustness of its Zr analogue *in vivo*[11,12], 343HOPO appears to be an excellent candidate for biological applications involving the chelation of Hf(IV).

For the sake of comparison with the larger group IV elements, interactions between 343HOPO and Ti(IV) in aqueous solution were also probed. Complex formation was evidenced by an intense ligand-to-metal charge (LMCT) band giving rise to a yellow coloration immediately after mixing the metal ion and 343HOPO (Figure S3). The LMCT band is centered at 381 nm and extends up to 500 nm. Formation of similar LMCT bands or yellow coloration has been previously noted for Ti(IV) complexes of hexadentate desferrioxamine B (DFO-B)[33] and bidentate 1,2-HOPO[34] - two ligands that belong to the same hydroxamate siderophore family as 343HOPO.

Surprisingly, 343HOPO was found to have much lower affinity for Ti(IV) than for Zr(IV) and Hf(IV). As shown in Figure S4, upon addition of Zr(IV) to an equimolar solution of 343HOPO and Ti(IV), the intense LMCT band decreases linearly until it totally disappears when the ratio Zr/343HOPO reaches 1 eq, indicating a total transmetallation reaction. In other word, the Ti(IV)-343HOPO species are, at least, 3 orders of magnitude less stable than [Zr^{IV}343HOPO]. In the presence of stoichiometric amount of bidentate 1,2-HOPO chelator, Uppal et al.[34] isolated the hexacoordinated complex [$Ti^{IV}(1,2\text{-HOPO})_2(OCH_3)_2$] as well as a dimeric heptacoordinated complex [$(1,2\text{-HOPO})_3TiOTi(1,2\text{-HOPO})_3$]. In the case of 343HOPO, its octacoordinating nature inherently creates a mismatch with the typical hexacoordinated geometry of Ti(IV) and probably impairs the formation of a more stable species. Such mismatch between 343HOPO and Ti(IV) also generates several possibilities for coordinating Ti(IV) to six out of eight 1,2-HOPO oxygens and leaves some of them available for protonation. Furthermore, the very small ionic radius of Ti(IV) (0.61 Å if CN = 6 or 0.74 Å if CN = 8)[35] is not optimal for the large binding cavity of 343HOPO, which certainly lowers the stability of this metal-ligand assembly. In line with these facts, all crystallization tests with Ti(IV) and 343HOPO failed. Taking into account these observations, and due to the complex hydrolytic behavior of Ti(IV), no further attempt was made to decipher the complicated speciation of the Ti(IV)-343HOPO system.

Selectivity of 343HOPO. Fig. 2 compares the stability constants of octacoordinated complexes of tetravalent and trivalent cations with 343HOPO as well as with two chelators widely used for d-block metals, namely EDTA and DTPA.

For the three chelators, increased log β values are observed from La^{3+} to Lu^{3+}, with a marked increase in the case of 343HOPO, suggesting that the binding energy trend overcomes the lanthanide hydration energy trend across the series.[36] The results obtained in the present study, confirm the preference of 343HOPO for octacoordinated tetravalent cations across the periodic table with formation of extremely stable complexes regardless of their size – from small Hf^{4+} (0.83 Å) to the 27 % bigger Th^{4+} (1.05 Å). While the stability of DTPA and EDTA complexes decreases by 6.7 and 6.3 orders of magnitude going from Hf(IV) to Th(IV), respectively, 343HOPO complexes with Hf and Th complexes are only 2.2 orders of magnitude apart. Furthermore, 343HOPO has a remarkable M(IV)/M(III) selectivity. As such, log β_{110} for $[Lu^{III}343HOPO]^-$ is only[7] 21.2, which translates to a selectivity of $10^{21.1}$ toward Hf over Lu - two adjacent elements of the periodic table. By comparison, the stability ratio between Hf(IV) and Lu(III) is only 10^{13} and $10^{9.8}$ for the DTPA and EDTA systems, respectively.

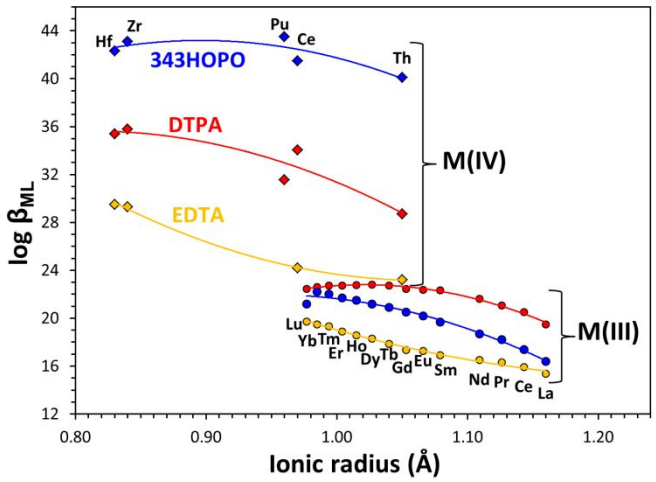

Fig. 2 Comparison of the selectivity of 343HOPO (blue points), DTPA (red points), and EDTA (yellow points) towards tetravalent metal ions (diamonds) and trivalent lanthanides (circles). Ionic radii of the cations are for a coordination number of 8 and were taken from Shannon.[35] Log β_{110} values for EDTA and DTPA were taken from the NIST Critical database[22]. Values for 343HOPO were taken from Sturzbecher-Hoehne et al.[7] and Deblonde et al.[9]

The ability of 343HOPO to form highly stable complexes with both trivalent and tetravalent ions, while retaining an incredible charge-based selectivity, is consistent with recent DFT calculations.[37] Kelley et al. found that the hydroxypyridinone rings of 343HOPO play a central role in this selectivity, as they are capable of both accepting and donating electron density. Such a property is evidently lacking in the simple carboxylate groups of EDTA or DTPA.

The high selectivity Hf/Lu of 343HOPO can certainly be leveraged in separation processes for the production of carrier-free ^{177}Lu, a radioisotope that is used in targeted radioimmunotherapy and decays to stable ^{177}Hf. The incredible charge-based and denticity-driven selectivity of 343HOPO is observed across the periodic table and suggests that this particular chelator could be an excellent stabilizer of rarely studied octacoordinated tetravalent cations such as Rf(IV) - the last group IV member. The simple and robust speciation of 343HOPO complexes would allow sequestering and purifying the short-lived isotopes of Rf (maximum half-life of 13.1 h for Rf-265) once it becomes available for molecular chemistry experiments. More realistically, the last naturally occurring octacoordinated tetravalent cation that has not been investigated with 343HOPO is Po(IV) (ionic radius of 1.08 Å)[35]. There is currently a lack of efficient decorporation agents for toxic polonium isotopes. It has been proven[38] that DTPA is a relatively weak chelator for Po(IV) but given the 7-10 orders of magnitude difference between the M(IV) complexes of 343HOPO and DTPA (Fig. 2), the former is predicted to strongly bind Po(IV). Furthermore, the efficacy of 343HOPO for radioisotope decorporation is well established,[39] which makes it a candidate of choice for development of future Po contamination countermeasures.

The selectivity of 343HOPO among its complexes with tetravalent metals was also observed via reverse phase liquid chromatography (Fig. 3). This type of selectivity is based on polarity differences among the species rather than their thermodynamic stability. Elution of the Zr, Hf, and Sn complexes was performed on an octadecyl (C-18) column using free 343HOPO as an internal reference. The retention times of the three complexes were as follows: 16.24 min for $[Sn^{IV}343HOPO]$, 16.29 min of $[Hf^{IV}343HOPO]$ and 16.39 min for $[Zr^{IV}343HOPO]$.

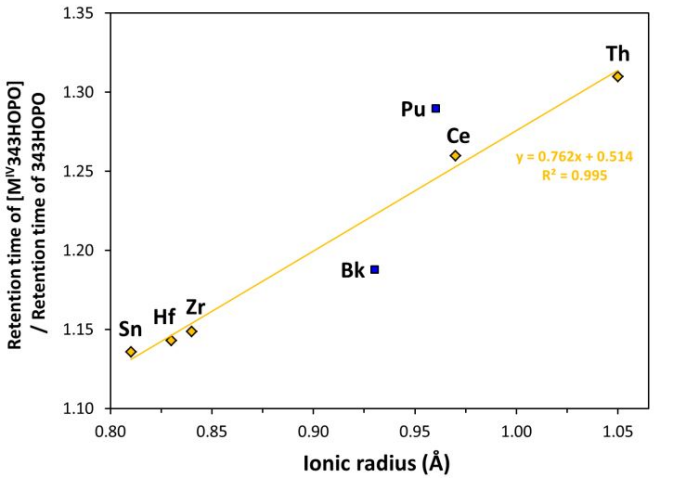

Fig. 3 Retention times of the M(IV) complexes of 343HOPO relative to the retention time of the free ligand as a function of the ionic radius of the cations (CN = 8). C18 column. Data for Ce(IV), Th(IV), Pu(IV), and Bk(IV) were taken from the literature [8,10].

These results indicate that $[Hf^{IV}343HOPO]$ is less polar than its Zr counterpart. The difference between the Zr and Hf complexes is noticeable as the separation of these two elements is known to be particularly arduous, even from an analytical chemistry stand point[40].

Building on the body of data on 343HOPO available in the literature, Fig. 3 compiles the relative retention times of its octacoordinated tetravalent complexes as a function of the cation ionic radius. Decreased polarity for these neutral complexes is observed when the ionic radius of the metal ion increases. The following trend in polarity is observed: Sn > Hf > Zr > Bk > Ce > Th. Based on the observed trend, $[Po^{IV}343HOPO]$

(ionic radius of 1.08 Å for CN of 8)[35] should have the longest retention time and be easily separated from all other tetravalent cations using a conventional C-18 column, opening avenues for polonium nuclear forensic analyses using 343HOPO.

Interestingly, the relative retention time increases linearly with the ionic radius only for the cations that do not have an open 5-f shell. The examples that do not follow this trend are the tetravalent cations with an open f-shell, namely Pu ($5f^4$) and Bk ($5f^7$). It is not clear at this point if this effect is due to participation of the 5f electrons in bonding within [Pu^{IV}343HOPO] and [Bk^{IV}343HOPO], which could influence their electronic structure and polarity.

Regarding the transactinide Rf(IV), its predicted ionic radius for a CN of 6 (the one for CN of 8 has not been published)[41,42] is between 0.74 and 0.79 Å. This range is bigger than the ionic radius of hexacoordinated Zr(IV) (0.72 Å) but smaller than that of Bk(IV) (0.83 Å). With this situation, [Rf^{IV}343HOPO] would be easily isolated from other [M^{IV}343HOPO] complexes (Figure S5) and the measurement of its retention time would indicate if it behaves more like a d-block or an f-block element.

The present results highlight that the selectivity of 343HOPO is three-fold: i) it has an extreme charge-based selectivity toward tetravalent cations, ii) it has a higher affinity toward octacoordinated cations, and iii) it is also capable of discriminating between cations of the same class. These remarkable properties are currently being studied for the development of highly-selective separation processes.

Acid resistance of group IV metal complexes with 343HOPO. The robustness of group IV complexes of 343HOPO toward acid attack was also investigated. Fig. 4 displays the UV-vis absorbance spectra of the Ti(IV), Zr(IV), and Hf(IV) complexes in highly concentrated HCl up to 10 M. The Hf and Zr complexes show exceptional robustness with no change in their UV-vis spectra up to 6 M HCl and very minimal changes from 6 to 10 M HCl (Fig. 4 and Figure S6). The Ti-343HOPO spectrum exhibit more variations with increasing proton concentration. A blue shit of the π-π* transition from 297 to 286 nm was observed as well as an increase in its extinction coefficient by about 80 %. This is consistent with protonation of one of the four chelating units of 343HOPO, which is likely not bound to Ti(IV) due to its preferred hexacoordination. Nonetheless, the MLCT band characteristic of the Ti complex persists, with only a minimal shift from 381 to 377 nm, indicating that 343HOPO is still bound to Ti(IV) even in 10 M HCl. Acidic samples of Ti-, Zr-, or Hf-343OHPO were found stable at room temperature for weeks highlighting the exceptional robustness of this chelator.

On the other side of the acidity scale, the resistance of tetravalent 343HOPO species against hydrolysis had not been experimentally probed in detail. For comparison, in the absence of chelator, Zr(IV) and Hf(IV) are hydrolyzed even at pH lower than 1 (Figure S7).

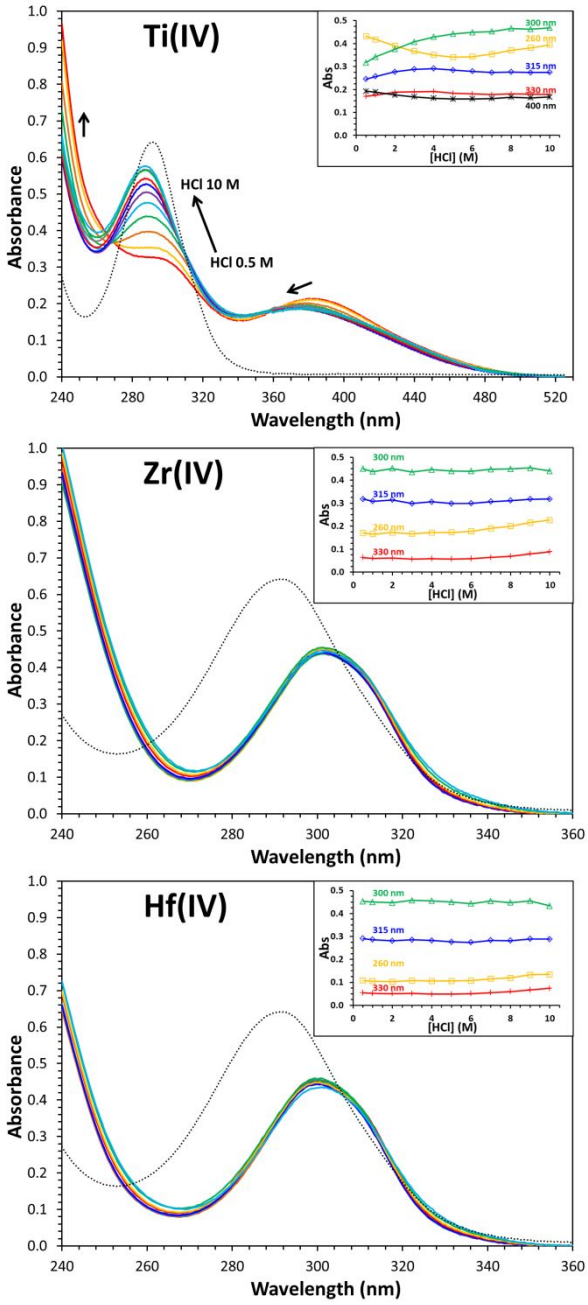

Fig. 4. UV-vis spectra of HCl solutions (0.5 to 10 M) containing 1 eq. of 343HOPO and 1 eq. of Ti(IV), Zr(IV), or Hf(IV). The spectrum of the free ligand in 6 M HCl (dotted line) is given for comparison. Insets: Absorbance at 260 (squares), 300 (triangles), 315 (diamonds) and 330 (crosses), and 400 nm (stars) as a function of HCl concentration. See Figure S 5 for more details.

As shown in Fig. 5, [Hf^{IV}343HOPO] and [Zr^{IV}343HOPO] also exhibit excellent robustness in basic media with Zr(IV) and Hf(IV) remaining stable with respect to hydrolytic precipitation up to pH ~10.7. These results are in excellent agreement with the pH release value predicted from the stability constant of [Hf^{IV}343HOPO] and [Zr^{IV}343HOPO] determined in acidic media (Figure S7). The chelation of hard Lewis acids like Zr(IV) and Hf(IV) ions over an acidity range so wide (from 10^{-10} to 10 M H^+)

is, to the best of our knowledge, not seen in any other type of chelator.

Regarding the Ti(IV) species with 343HOPO, they were found to be less resistant to hydrolysis than their Zr and Hf analogues. The characteristic LMCT band center at 380 nm disappears at pH above ~6 and hydrolytic precipitation was observed.

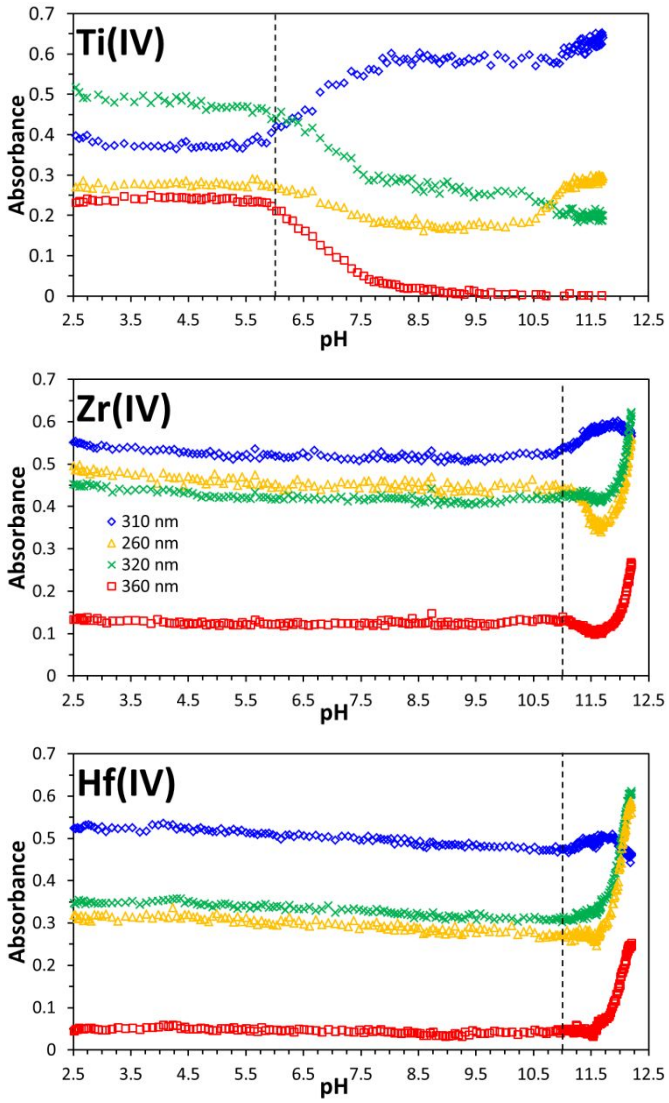

Fig. 5. UV-vis absorbance of the Ti(IV)-HOPO (top), Zr(IV)-HOPO (middle) and Hf(IV)-HOPO (bottom) systems at relevant wavelengths and as a function of pH. Yellow triangles: 260 nm. Blue diamonds: 310 nm. Green crosses: 320 nm. Red squares: 360 nm. [Metal] = [343HOPO]. T = 25°C. The dotted line delineates the precipitation of hydroxide species.

This behavior is consistent with the lower stability of the Ti(IV) species relative to their Zr(IV) and Hf(IV) counterparts observed in HCl media (*vide supra*). Based on the different precipitation pH between Ti(IV) and Zr(IV) or Hf(IV) in the presence of 343HOPO (6 vs. 10.7), simple but selective separation methods for group IV elements could be envisioned.

Structural characterization and chirality of 343HOPO complexes. Despite the plethora of studies focusing on 343HOPO and its promising use in a variety of applications such as actinide decorporation[39], post-MRI chelation therapy[43], ^{89}Zr PET imaging[11,12], or separation processes, structural information on this molecule and its complexes has remained scarce. Thus far, only three crystal structures containing 343HOPO have been reported. The structure of the unchelated ligand is also still unknown. In 2015, Daumann et al.[44] first reported the structure of [KEu^{III}343HOPO]·DMF (obtained by vapor diffusion of ethyl ether into a DMF solution). That same year, Deri et al. reported the single crystal structure of [Zr^{IV}343HOPO]·$(MeOH)_{2.43}$·$(H_2O)_{0.79}$, obtained by slow cooling of an oversaturated solution in methanol.

More recently, we obtained single crystals of [Sn^{IV}343HOPO]·$3H_2O$, which crystallized (by slow evaporation of a methanol solution) in the chiral orthorhombic space group $C222_1$. While it is possible for achiral molecules to crystallize in chiral space groups (especially if solvent is included in the lattice), we found the Sn(IV) 343HOPO complex itself was the cause of this chirality. This complexation-induced chirality, which is often observed in metal chelator complexes, arises from the fact a metal ion can attack the ligand from two different sides, as shown in Scheme 1. The helical arrangement of 1,2-HOPO units in the Sn(IV) 343HOPO crystal selected for analysis were found to bind to the metal to form a square antiprism, and orient themselves with a Λ handedness: moreover, the backbone of 343HOPO contains a central butylene diamine chain plus two C3 sidechains, which were found to arrange with a Δ handedness. Overall, this leads to an assignment of the chirality of the Sn(IV) complex as Λ(δ), which denotes both components of helical handedness in this molecule. Presumably, the formation of the corresponding Δ(λ) enantiomer is equal in solution, and also crystallizes in the same chiral space group.

These observations inspired us to analyze other previously reported crystal structures of 343HOPO complexes, and we found that the same complexation-induced enantiomery is also apparent in achiral space groups, where racemic mixtures of the Λ(δ) and Δ(λ) enantiomers are present in the unit cells of both [KEu^{III}343HOPO]·DMF and Zr^{IV}343HOPO]·$(MeOH)_{2.43}$·$(H_2O)_{0.79}$ (Fig. 6). Thus, a single, structurally analogous set of enantiomers is observed in the structures of 343HOPO complexes with Sn^{IV}, Zr^{IV}, and Eu^{III}. Moving on to the present case of Hf, we found the crystallization procedure reported for the Zr analogue did not yield any crystalline material, however single crystals of [Hf^{IV}343HOPO]·$3H_2O$ could be obtained by slow evaporation of a wet ethanol solution. Akin to its Sn^{IV} analog, [Hf^{IV}343HOPO] crystallizes in the chiral space group $C222_1$, however serendipitously, the crystal selected for analysis displayed the Δ(λ) enantiomer. Depictions of the structurally-related Sn^{IV}, Hf^{IV}, and Zr^{IV} 343HOPO complexes can be seen in Figure 6. An ellipsoid plot of the Zr^{IV} 343HOPO structure is provided in supporting Figure S9.

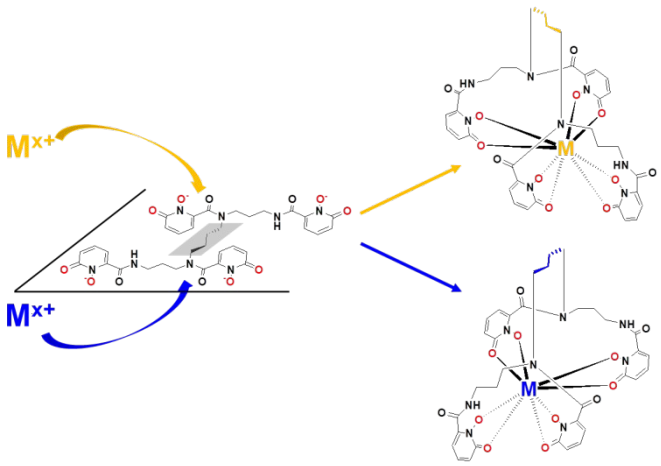

Scheme 1. Formation of two enantiomers starting from the achiral ligand 343HOPO. The Λ(δ) conformation is highlighted in yellow. The Δ(λ) conformation is highlighted in blue. Some bonds are elongated for clarity.

Based on the accumulated structural data of 343HOPO complexes, we posit that the well-defined chirality of these species may provide a basis for several unique experiments. Considering studies of 343HOPO are frequently inspired by its potential biomedical applications, notably for metal decorporation, it would be useful to determine if the chirality of metal 343HOPO complexes plays a discriminatory role *in vivo*. To this end, we believe that the extremely high stability constants of tetravalent metal complexes with 343HOPO would allow for a chiral chromatographic separation of their enantiomeric conformers, allowing for their distinct biological activities to be probed. Additionally, the preparation of enantiomerically pure samples of 343HOPO complexes would permit the measurement of their optical rotation properties, which may provide a new means of measuring stability constants on the basis of their rates of racemization. In all, the indication that 343HOPO complexes form a single set of well-defined enantiomers, coupled with their extreme stabilities and biomedical relevance, may provide the basis for several unique experiments.

Conclusions

The results obtained in the present study show that tetravalent complexes of 343HOPO exhibit extreme stability in solution. Octacoordinated [Hf^{IV}343HOPO] and [Zr^{IV}343HOPO] were found particularly stable (log β_{110} > 42) and resistant to both acid and hydroxide attack with formation of the two complexes between pH 10 and 10 M HCl. The equivalent Ti(IV) system was found to be far less stable (hydrolyzed at pH > 6) suggesting a hexacoordinated environment. The selectivity of 343HOPO was observed at three levels: i) extreme affinity for tetravalent cations, ii) preference for octacoordinated complexes, and iii) polarity discrimination among complexes of the same class. This makes 343HOPO a potential candidate for selective chelation of the sparsely-studied Po(IV) and Rf(IV) ions. Furthermore, the solid-state chemistry of 343HOPO has indicated the formation of a single set of two enantiomers upon metal chelation, which may provide a useful basis for future biological and kinetic studies following a chromatographic separation of these enantiomers.

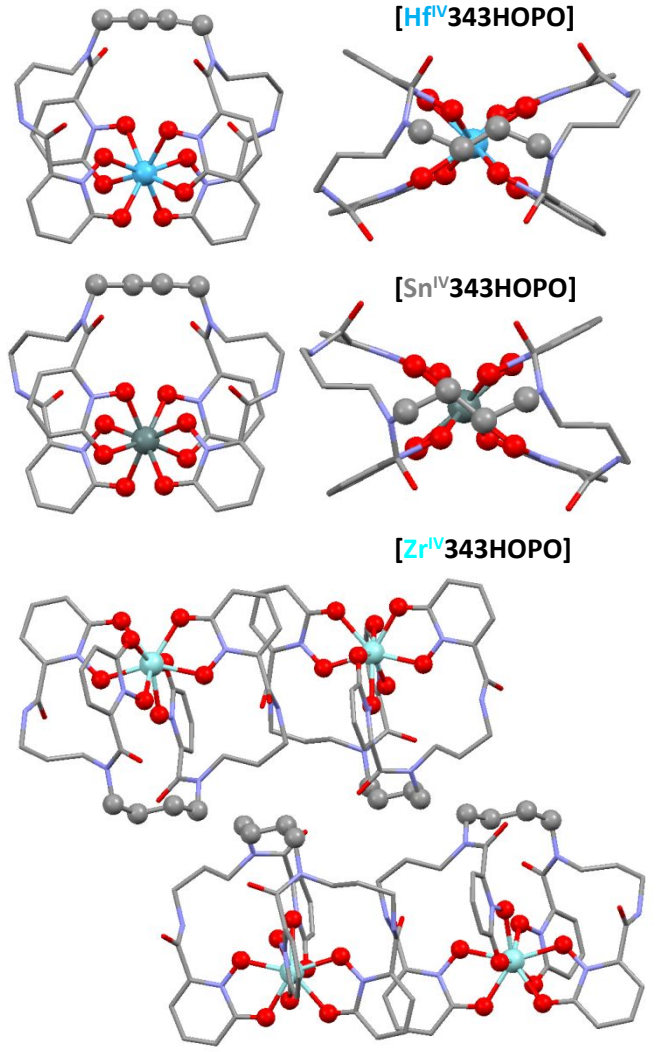

Fig. 6 Representation of the crystal structure of 343HOPO complexes with Hf(IV) (top), Sn(IV) (center), and Zr(IV) (bottom). The 4-carbon chain of the ligand's backbone (grey), the coordinating oxygen atoms (red), and the metal centre Hf (light blue), Sn (grey), or Zr (cyan) are displayed as spheres. As depicted, [Sn343HOPO] exhibits the Λ(δ) conformation whereas [Hf343HOPO] exhibits the Δ(λ) conformation. [Zr343HOPO] is depicted in both conformations, as seen in the unit cell.

Conflicts of interest

There are no conflicts to declare.

Acknowledgements

This work was supported by the U.S. Department of Energy (DOE), Office of Science, Office of Basic Energy Sciences, Chemical Sciences, Geosciences, and Biosciences Division at LBNL, under contract No. DE-AC02-05CH11231.The ALS is supported by the U.S. DOE, Office of Science, Office of Basic Energy Sciences, under Contract No. DE-AC02-05CH11231. The authors thank Dr. Simon J. Teat of ALS station 11.3.1 for training and guidance throughout our single crystal X-ray diffraction

studies. T.D.L. thanks the U.S. DOE Integrated University Program for a graduate research fellowship.

Notes and references

1 A. E. V. Gorden, J. Xu, K. N. Raymond and P. Durbin, *Chemical Reviews*, 2003, **103**, 4207–4282.
2 D. L. White, P. W. Durbin, N. Jeung and K. N. Raymond, *J. Med. Chem.*, 1988, **31**, 11–18.
3 M. Sturzbecher-Hoehne, G. J.-P. Deblonde and R. J. Abergel, *Radiochimica Acta*, 2013, **101**, 359–366.
4 G. J.-P. Deblonde, T. D. Lohrey, D. D. An and R. J. Abergel, *New Journal of Chemistry*, 2018, **42**, 7649–7658.
5 M. Sturzbecher-Hoehne, B. Kullgren, E. E. Jarvis, D. D. An and R. J. Abergel, *Chemistry - A European Journal*, 2014, **20**, 9962–9968.
6 M. Sturzbecher-Hoehne, P. Yang, A. D'Aléo and R. J. Abergel, *Dalton Transactions*, 2016, **45**, 9912–9919.
7 M. Sturzbecher-Hoehne, C. Ng Pak Leung, A. D'Aléo, B. Kullgren, A.-L. Prigent, D. K. Shuh, K. N. Raymond and R. J. Abergel, *Dalton Transactions*, 2011, **40**, 8340.
8 M. Sturzbecher-Hoehne, T. A. Choi and R. J. Abergel, *Inorganic Chemistry*, 2015, **54**, 3462–3468.
9 G. J.-P. Deblonde, M. Sturzbecher-Hoehne and R. J. Abergel, *Inorganic Chemistry*, 2013, **52**, 8805–8811.
10 G. J.-P. Deblonde, M. Sturzbecher-Hoehne, P. B. Rupert, D. D. An, M.-C. Illy, C. Y. Ralston, J. Brabec, W. A. de Jong, R. K. Strong and R. J. Abergel, *Nature Chemistry*, 2017, **9**, 843–849.
11 M. A. Deri, S. Ponnala, B. M. Zeglis, G. Pohl, J. J. Dannenberg, J. S. Lewis and L. C. Francesconi, *Journal of Medicinal Chemistry*, 2014, **57**, 4849–4860.
12 M. A. Deri, S. Ponnala, P. Kozlowski, B. P. Burton-Pye, H. T. Cicek, C. Hu, J. S. Lewis and L. C. Francesconi, *Bioconjugate Chemistry*, 2015, **26**, 2579–2591.
13 M. Berger, M. Bauser, T. Frenzel, C. S. Hilger, G. Jost, S. Lauria, B. Morgenstern, C. Neis, H. Pietsch, D. Sülzle and K. Hegetschweiler, *Inorg. Chem.*, 2017, **56**, 5757–5761.
14 T. Frenzel, M. Bauser, M. Berger, C. S. Hilger, C. Hegele-Hartung, G. Jost, C. Neis, K. Hegetschweiler, B. Riefke, D. Suelzle and H. Pietsch, *Investigative Radiology*, 2016, **51**, 776.
15 A. Dash, M. R. A. Pillai and F. F. Knapp, *Nucl Med Mol Imaging*, 2015, **49**, 85–107.
16 D. V. Filosofov, N. S. Loktionova and F. Rösch, *Radiochimica Acta*, 2010, **98**, 149–156.
17 R. Hernandez, H. F. Valdovinos, Y. Yang, R. Chakravarty, H. Hong, T. E. Barnhart and W. Cai, *Mol. Pharmaceutics*, 2014, **11**, 2954–2961.
18 K. Ishiwata, T. Ido, M. Monma, M. Murakami, H. Fukuda, M. Kameyama, K. Yamada, S. Endo, S. Yoshioka, T. Sato and T. Matsuzawa, *International Journal of Radiation Applications and Instrumentation. Part A. Applied Radiation and Isotopes*, 1991, **42**, 707–712.
19 R. J. Abergel, P. W. Durbin, B. Kullgren, S. N. Ebbe, J. Xu, P. Y. Chang, D. I. Bunin, E. A. Blakely, K. A. Bjornstad, C. J. Rosen, D. K. Shuh and K. N. Raymond, *Health Physics*, 2010, **99**, 401–407.
20 P. Gans and B. O'Sullivan, *Talanta*, 2000, **51**, 33–37.
21 P. Gans, A. Sabatini and A. Vacca, *Talanta*, 1996, **43**, 1739–1753.
22 A. E. Martell, R. M. Smith and R. J. Motekaitis, .
23 Organisation for Economic Co-operation and Development, *Chemical Thermodynamics of Tin - Volume 12*, OECD Publishing, Paris, 2012.
24 F. J. Mompean, J. Perrone and M. Illemassène, *Chemical thermodynamics of zirconium*, Gulf Professional Publishing, 2005, vol. 8.
25 Bruker, *SADABS, APEX3, and SAINT*, Bruker AXS, Madison, Wisconsin, USA.
26 G. M. Sheldrick, *Acta Crystallographica Section A Foundations of Crystallography*, 2008, **64**, 112–122.
27 L. J. Farrugia, *Journal of Applied Crystallography*, 2012, **45**, 849–854.
28 C. F. Macrae, P. R. Edgington, P. McCabe, E. Pidcock, G. P. Shields, R. Taylor, M. Towler and J. van de Streek, *J Appl Cryst*, 2006, **39**, 453–457.
29 Y. Suzuki, T. Nankawa, A. J. Francis and T. Ohnuki, *Radiochimica Acta*, , DOI:10.1524/ract.2010.1735.
30 M. A. Brown, A. Paulenova and A. V. Gelis, *Inorganic Chemistry*, 2012, **51**, 7741–7748.
31 E. G. Moore, J. Xu, C. J. Jocher, E. J. Werner and K. N. Raymond, *Journal of the American Chemical Society*, 2006, **128**, 10648–10649.
32 A. D'Aléo, E. G. Moore, J. Xu, L. J. Daumann and K. N. Raymond, *Inorg. Chem.*, 2015, **54**, 6807–6820.
33 K. E. Jones, K. L. Batchler, C. Zalouk and A. M. Valentine, *Inorg. Chem.*, 2017, **56**, 1264–1272.
34 R. Uppal, H. P. Israel, C. D. Incarvito and A. M. Valentine, *Inorganic Chemistry*, 2009, **48**, 10769–10779.
35 R. Shannon, *Acta Crystallographica Section A*, 1976, **32**, 751–768.
36 M. Regueiro-Figueroa, D. Esteban-Gómez, A. de Blas, T. Rodríguez-Blas and C. Platas-Iglesias, *Chemistry - A European Journal*, 2014, **20**, 3974–3981.
37 M. P. Kelley, G. J.-P. Deblonde, J. Su, C. H. Booth, R. J. Abergel, E. R. Batista and P. Yang, *Inorganic Chemistry*, 2018, **57**, 5352–5363.
38 A. Younes, G. Montavon, S. G. Gouin, E. André-Joyaux, R. Peumery, T. Chalopin, C. Alliot, M. Mokili, J. Champion and D. Deniaud, *Chemical Communications*, 2017, **53**, 6492–6495.
39 D. D. An, B. Kullgren, E. E. Jarvis and R. J. Abergel, *Chemico-Biological Interactions*, 2017, **267**, 80–88.
40 M. Smolik, A. Jakóbik-Kolon and M. Porański, *Hydrometallurgy*, 2009, **95**, 350–353.
41 A. Bilewicz, *Radiochimica Acta*, 2000, **88**, 833–835.
42 E. Johnson and B. Fricke, *J. Phys. Chem.*, 1991, **95**, 7082–7084.
43 J. A. Rees, G. J.-P. Deblonde, D. D. An, C. Ansoborlo, S. S. Gauny and R. J. Abergel, *Scientific Reports*, , DOI:10.1038/s41598-018-22511-6.
44 L. J. Daumann, D. S. Tatum, B. E. R. Snyder, C. Ni, G. Law, E. I. Solomon and K. N. Raymond, *Journal of the American Chemical Society*, 2015, **137**, 2816–2819.

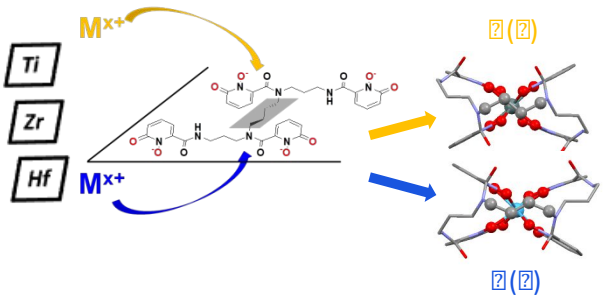

Hydroxypyridinone ligand 3,4,3-LI(1,2-HOPO) exhibits remarkable charge-based selectivity for octacoordinated tetravalent cations, forming stable chiral complexes over a very broad pH range.